Model Based Flowsheet Studies on Cement Clinker Production Processes

George Melitos[a,b], Bart de Groot[a]*, Fabrizio Bezzo[b]

[a] Siemens Industry Software Limited, 26-28 Hammersmith Grove, W6 7HA London, United Kingdom
[b] CAPE-Lab (Computer-Aided Process Engineering Laboratory), Department of Industrial Engineering, University of Padova, 35131 Padova PD, Italy
* Corresponding Author: b.degroot@siemens.com

ABSTRACT

Clinker is the main constituent of cement, produced in the pyroprocessing section of the cement plant. This comprises some high temperature and carbon intensive processes, which are responsible for the vast majority of the CO_2 emissions associated with cement production. This paper presents first-principles mathematical models for the simulation of the pyroprocess section; more specifically the preheating cyclones, the calciner and the rotary kiln. The models incorporate material and energy balances, the major heat and mass transport phenomena, reaction kinetics and thermodynamic property estimation models. These mathematical formulations are implemented in the gPROMS® Advanced Process Modelling Environment and the resulting index-1 DAE (Differential Algebraic Equation) system can be numerically solved for various reactor geometries and operating conditions.

The process models developed for each unit are then used to build a cement pyroprocess flowsheet model. The flowsheet model is validated against published data, demonstrating the ability to predict accurately operating temperatures, degree of calcination, gas and solid compositions, fuel consumption and overall CO_2 emissions. The substitution of conventional coal with more sustainable fuels is also investigated, to evaluate the potential for avoiding CO_2 emissions by replacing part of the fossil-based coal fuel (used as a reference case). Trade-offs between different process KPIs (f.e. calcination efficiency, specific CO_2 emissions per tonne of clinker) are identified and evaluated for each fuel utilization scenario.

Keywords: Mathematical Modelling, Cement Production, Simulation, Alternative Fuels, Decarbonisation

INTRODUCTION

The share of cement and concrete value chain to global CO_2 emissions is estimated at 6-7% [1]. These emissions originate from a series of several industrial activities. The first step is the extraction and mining of the raw materials, followed by the preparation and processing of them for the production of clinker, the main component of cement. Once clinker is formed, it is cooled and subsequently ground with gypsum and other additives to produce cement. Cement is then mixed with several aggregates, admixtures and water to form concrete. The stage responsible for the vast majority of the CO_2 emissions is the thermal processing (pyroprocessing) of the raw materials for the production of clinker.

The pyroprocessing section of a typical cement plant consists of four main processes: the preheating cyclones, the calciner, the rotary kiln and the grate cooler. From these processes, the calciner and the rotary kiln are responsible for almost 90% of the total emissions [2]. These two processes facilitate the chemical transformation of the raw materials into clinker. Specifically, in the calciner calcium carbonate (limestone) is decomposed into calcium oxide (lime) and carbon dioxide. This reaction is responsible for 60% of the total emissions, the so-called process emissions [1]. These emissions are unavoidable in principle since calcium oxide is the most important intermediate in the clinker formation process. After calcium oxide is formed it reacts with all the remaining raw materials (silicon dioxide, ferric oxide, alumina oxide)

to form the final clinker product inside the rotary kiln. Most of the chemical reactions described above are endothermic and require a substantial amount of heat, which is provided to the process by internal combustion of a solid fuel. The emissions due to fuel combustion are responsible for the remaining 40% of the carbon dioxide emissions [1].

The most common fuels used in the calciner, and the rotary kiln are the fossil-based pulverized coal or petcoke. However, the utilization of solid recovered fuels (SRF) is becoming a common practice in cement industry. These fuels originate from municipal solid waste processing and can play a crucial role in the mitigation of the direct CO_2 emissions of a cement plant. This is due to the high biogenic carbon content of such fuels, which emissions during combustion are considered neutral [3]. Based on their source and nature, alternative fuels have different chemical and mechanical properties which affect directly their performance upon combustion [4].

The chemical and physical phenomena occurring in the clinker production processes are rather complex and to this day, these processes have mostly been studied and modelled in literature as standalone unit operations. As a result, there is a lack of holistic model-based approaches on flowsheet simulations of cement plants in literature.

This work sets out to investigate the performance of the clinked production process in a holistic manner, utilizing mechanistic mathematical models. These are used to simulate a reference coal-fired cement plant, validated from literature data. Once the predictive ability of the models is verified, several case studies are presented in which different alternative fuels are used to replace coal, investigating the potential effect of fuel subtitution in the plant's emissions and performance.

METODOLOGY

Pyroprocess System Description

The pyroprocess system of a cement plant consists of the preheating cyclones, the calciner, the rotary kiln and the grate cooler. The solid raw meal feedstock is being heated inside the cyclones up to 800°C, then calcined in the calciner and finally converted into clinker reaching 1450°C inside the rotary kiln, while thermal energy from the hot clinker exiting the kiln is recovered in the cooler and recycled back to the former processes by the secondary air (to the kiln) and tertiary air (to the calciner) streams. A visual representation of the pyroprocessing system is presented in Figure 1. The mathematical modelling framework that has been developed and used to perform the simulations will be explained briefly. Given the greater potential for emission reduction, the study focuses on the carbon intensive processes (calciner, kiln) and the CO_2 reduction potential from alternative fuel combustion. These models are then used in a flowsheet simulation and the results are presented in the following Chapter.
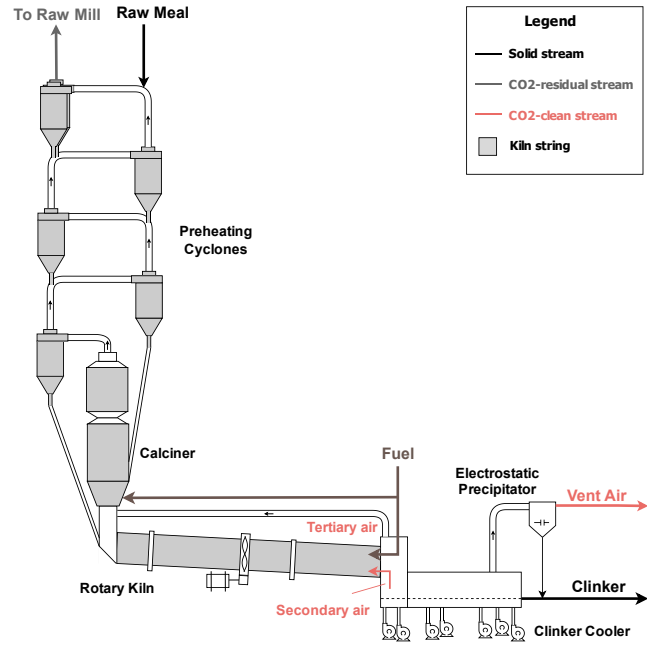

Figure 1: Cement Pyroprocess Plant (modified from [5]).

Preheating Cyclones

The preheating cyclones are modelled as a direct heat exchange process, in which the hot exhaust gas is mixed with the cold solid. The two streams exchange heat inside the cyclones and then are separated in the underflow (solids) and the overflow of the cyclone (gas with dust). Assuming steady state operation the material balance for the solid (1) and gas phase (2) and the energy balance (3) for each cyclone are written as:

$$m_{s,j-1} + m_{es,j+1} = m_{s,j} + m_{es,j} - m_{m,j} \quad \forall j \in 1, N \quad (1)$$

$$m_{g,j} = m_{g,j-1} + m_{fa,j} + m_{m,j} \quad \forall j \in 1, N \quad (2)$$

$$m_s C_{p,s} T\big|_{j-1} + m_{es} C_{p,s} T\big|_{j+1} + m_g C_{p,g} T\big|_{j-1} + m_{fa,j} C_{p,a} T_a$$
$$= m_s C_{p,s} T\big|_j + m_{es} C_{p,s} T\big|_j + m_g C_{p,g} T\big|_j$$
$$\forall j \in 1, N \quad (3)$$

Where $m_{i,j}$ (kg/s) is the mass flowrate of the phase i out of cyclone j, $Cp_{i,j}$ (J/kg*K) is the specific heat capacity of the phase i in cyclone j and T_j (K) is the temperature inside cyclone j. Regarding the phases i, s refers to the solid phase, g refers to the gas phase, es refers to the solids entrained by the gas, m refers to the moisture of the raw meal and fa refers to the false air that is entering each cyclone.

Except for the mass and energy balances reported above, sub-models for the estimation of the heat losses and pressure drops around each cyclone are included as well, following approaches from relevant literature works [6-7].
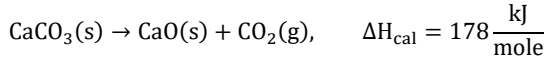
Calciner

The basis of the calciner model were general material and energy conservation balances:

$$\frac{dm_i(z)}{dz} = A_{calciner} * \sum_j R_{i,j}(z) \quad \forall \, i \in solid, fuel, gas \quad (4)$$

$$\frac{dH_t(z)}{dz} = A_{calciner} * \left(\Delta H_{cal} * R_{cal}(z) + \sum_c \Delta H_c * R_c(z)\right) (5)$$

where $m_i(z)$ (kg/s) is the specific mass flowrate of the component i in the axial position z, $A_{calciner}$ (m^2) is the cross sectional area of the calciner, H_t (kW) is the enthalpy of the mixture in the axial position z and $R_{i,j}(z)$ (kg/m^3*s) is the volumetric reaction rate of component i in reaction j.

The rate expression for calcination reaction reads:

$$CaCO_3(s) \rightarrow CaO(s) + CO_2(g), \qquad \Delta H_{cal} = 178 \frac{kJ}{mole}$$

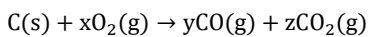$$R_{cal}(z) = k(z) * A_{CaCO_3}(z) * \rho_{CaCO_3} * \left(\frac{P_{eq}(z) - P_{CO_2}(z)}{P_{eq}(z)}\right) (6)$$

where $k(z)$ (kg/m^2) is the global calcination reaction constant, incorporating chemical and physical limitation terms [8], A_{CaCO3} (m^2/kg) is the specific surface area of the solids as a function of conversion [9], ρ_{CaCO3} (kg/m^3) is the solids density, $P_{eq}(z)$ (Pa) is the calcination equilibrium pressure [9] and P_{CO2} (Pa) the CO_2 partial pressure.

Regarding fuel combustion, there are multiple heterogeneous and homogeneous reaction steps occurring. The first step is the evaporation of the fuel moisture, followed by the devolatization of the volatile part of the fuel, leaving the solid particle with just char and ash. The rate expression $R_{i,dev}(z)$ for the devolatization follows an Arrhenius type behaviour:

$$R_{dev}(z) = A_{dev} * e^{-\frac{E_{dev}}{R*T_p}} \quad (7)$$

where T_p (K) is the particle temperature, R (kJ/mole*K) is the ideal gas constant and A_{dev} (1/s) and E_{dev} (kJ/mole) are the kinetic parameters, which are different for different types of solids fuels, like coal and SRF [5]. After the release of the volatiles in the gaseous phase, the volatile mixture that consists of CH_4, C_2H_4, H_2, CO, O_2, N_2 and S_2 is oxidized though homogeneous gas phase reactions to produce the oxidized form of these gases (CO_2, H_2O, NO, SO_2) and provide heat to the system. The kinetic rate expressions for each reaction are extracted from relevant literature [9]. The remaining char is reacting with oxygen according to the following reaction with the respective reaction rate $R_{char}(z)$:
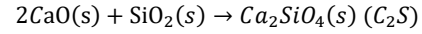
$$C(s) + xO_2(g) \rightarrow yCO(g) + zCO_2(g)$$

$$R_{char}(z) = \frac{A_p}{V_p} \frac{k_{chem}(z) * k_{phys}(z)}{k_{chem}(z) + k_{phys}(z)} P_{O_2}(z) \quad (8)$$
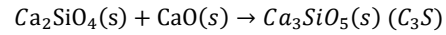
where x, y, z are temperature dependent coefficients, A_p (m^2) and V_p (m^3) are the particle's surface and volume, P_{O2} (Pa) is oxygen's partial pressure, and $k_{chem}(z)$ and $k_{phys}(z)$ (kg/m^2*Pa*s) are reaction constants, that are evaluated through expressions from literature [4,10].
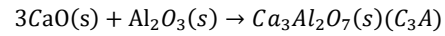
Rotary Kiln

For the rotary kiln system, the process model is divided into three sub-models that refer to: a) the motion of solid bed inside the rotating drum, b) the heat transfer phenomena between the solid bed, gas phase and rotating wall and shell, c) the chemical reactions occurring during clinkerization and fuel combustion. The first sub-model is used to calculate accurately the height of the bed, the residence time and velocity of the solids inside the kiln and the cross sectional and contact areas between the bed-gas-wall system, that are essential for the heat transfer model calculations. Due to page limitations the equations of these sub-models will not be displayed here, however the reader is referred to relevant literature works for both the bed motion [11] and heat transfer models [12-13]. For the chemical reaction sub-model, the four main clinker formation reactions were assumed, with the following kinetic rate expressions [13]:
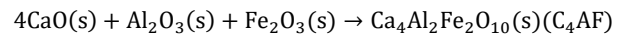
$$2CaO(s) + SiO_2(s) \rightarrow Ca_2SiO_4(s) \; (C_2S)$$

$$R_{C_2S}(z) = \rho_{bed} * k_{C_2S}(z) * y_{CaO}^2 * y_{SiO_2}$$

$$Ca_2SiO_4(s) + CaO(s) \rightarrow Ca_3SiO_5(s) \; (C_3S)$$

$$R_{C_3S}(z) = \rho_{bed} * k_{C_3S}(z) * y_{C_2S} * y_{CaO}$$

$$3CaO(s) + Al_2O_3(s) \rightarrow Ca_3Al_2O_7(s)(C_3A)$$

$$R_{C_3A}(z) = \rho_{bed} * k_{C_3A}(z) * y_{CaO}^3 * y_{Al_2O_3}$$

$$4CaO(s) + Al_2O_3(s) + Fe_2O_3(s) \rightarrow Ca_4Al_2Fe_2O_{10}(s)(C_4AF)$$

$$R_{C_4AF}(z) = \rho_{bed} * k_{C_4AF}(z) * y_{CaO}^4 * y_{Al_2O_3} * y_{Fe_2O_3}$$

where ρ_{bed} (kg/m^3) is the bed density, and k_i (1/s) and y_i (-) are the kinetic constants and mass fractions.

Following the common notation for the clinker phases in cement science, C_2S, C_3S, C_3A and C_4AF refer to Ca_2SiO_4, Ca_3SiO_5, $Ca_3Al_2O_7$ and $Ca_3Al_2Fe_2O_7$ respectively.

RESULTS & DISCUSSION

Base Case Coal Fired Simulation Results

In this part of the study, the models presented above will be solved simultaneously in a flowsheet simulation and the results will be validated against published data from a relevant work that is based on a cement process simulator developed by VDZ (Association of German Cement Works) [14]. The specification of all the inlet conditions were tuned in accordance with the literature source that was used to validate the results. The inlet

conditions and properties of the raw meal and fuel inlet streams are presented in Table 1. The equipment design was taken identical as the one from the reference source [14]. The preheating tower string consists of 5 cyclones and a calciner with a diameter of 3.88m and a length of 45m, while the kiln is 57m long with a diameter of 4.04m.

The results obtained from the simulation environment of gPROMS® were compared with the reference dataset, and the most important information is summarised in Table 2 and Figure 2. Starting from Table 2, the temperature predictions of the solid and gas streams around the cyclones-calciner string seem to align with the literature data, while the degree of calcination in the calciner is predicted accurately with a relative error of 0.5%.

Table 1: Raw Meal & Fuel Inlet Conditions.

Raw Meal Conditions		
Temperature (^{o}C)	60	
Mass Flowrate (kg/s)	55.2	
$CaCO_3$ (wt.% dry basis)	78.7	
SiO_2 (wt.% dry basis)	13.6	
Al_2O_3 (wt.% dry basis)	4.3	
Fe_2O_3 (wt.% dry basis)	2.4	
CaO (wt.% dry basis)	0.0	
Moisture (wt.%)	1.0	
Fuel Conditions	**Coal**	**SRF**
Temperature (^{o}C)	60	60
Mass Flowrate to Calciner (kg/s)	2.42	2.85
Mass Flowrate to Rotary Kiln (kg/s)	1.40	-
Fixed Carbon (wt.% wet basis)	51.0	10.0
Volatile Matter (wt.% wet basis)	32.0	69.3
Ash (wt.% wet basis)	16.5	13.8
Moisture (wt.% wet basis)	0.5	6.9
C (wt.% dry basis)	69.5	45.2
H (wt.% dry basis)	4.0	7.0
O (wt.% dry basis)	9.0	33.0
S (wt.% dry basis)	0.5	0.1
N (wt.% dry basis)	0.5	0.0

Table 2: Comparison of Model Predictions from Literature Data [14].

Variables	gPROMS	VDZ
Flue Gas Temperature (^{o}C)	315	314
Preheated Solids Temperature (^{o}C)	762	760
Calciner Gas Temperature (^{o}C)	865	864
Kiln Feed Loss on Ignition (%)	2.9	3.2
Degree of Calcination (%)	94.5	94.0

Moving onto the kiln system, it can be observed from Figure 2 that the prediction of the clinker phases composition is quite close to the reference data. Specifically, the mass fractions of C_3S and free lime are predicted precisely, while the simulated mass fractions of C_2S, C_3A and C_4AF deviate from the reference data with relative errors of 3.5%, 3.9% and 4.5% respectively.
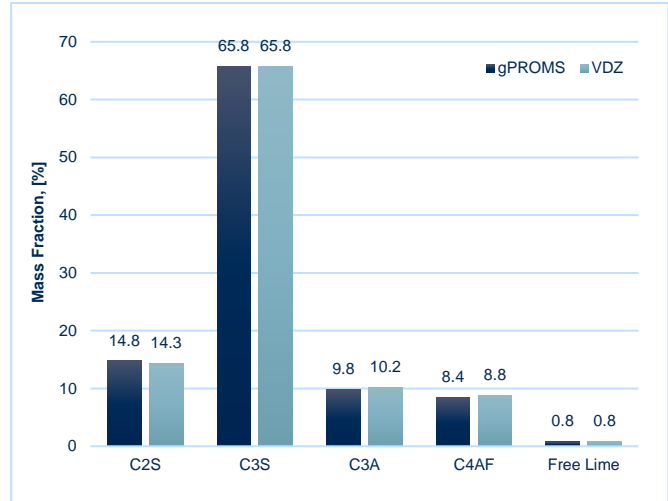

Figure 1: Model Predictions of Clinker Compositon.

Coal Substitution with Solid Recovered Fuels

The chemical (ultimate analysis, composition) and physical (proximate analysis, particle size) characteristics of the simulated SRF were extracted from relevant literature works and are presented in Table 1 [5,14]. Two different case studies were investigated, in which different average particle sizes were assumed. In the first case (SRF-1) a very fine SRF was assumed with an average particle size of 250 μm [5]. In the second case (SRF-2) a SRF with average particle size of 750 μm was assumed [12]. The target is to re-design the calciner system, by modifying the residence time, in order to achieve complete fuel combustion and reach the same temperature and degree of calcination in the outlet of the reactor, since these two variables are the most important KPIs for the operation of the calciner. The biogenic content of the SRFs is assumed to be 80%.

As presented in Figure 3, the temperature and calcination profiles for the three cases are quite different, since the fuels used in each case have different properties that result to different combustion behaviour. That being said, it is important to highlight that no matter the variability of the temperature and calcination distributions for each case study, the values of the variables in the outlet of the calciner have been kept almost the same by modifying the residence time from 2.9 seconds for the base case to 3.3 seconds and 4.1 seconds for the SRF-1 and 2 cases respectively. This translates to a larger calciner with an increased cross-sectional area (diameter),
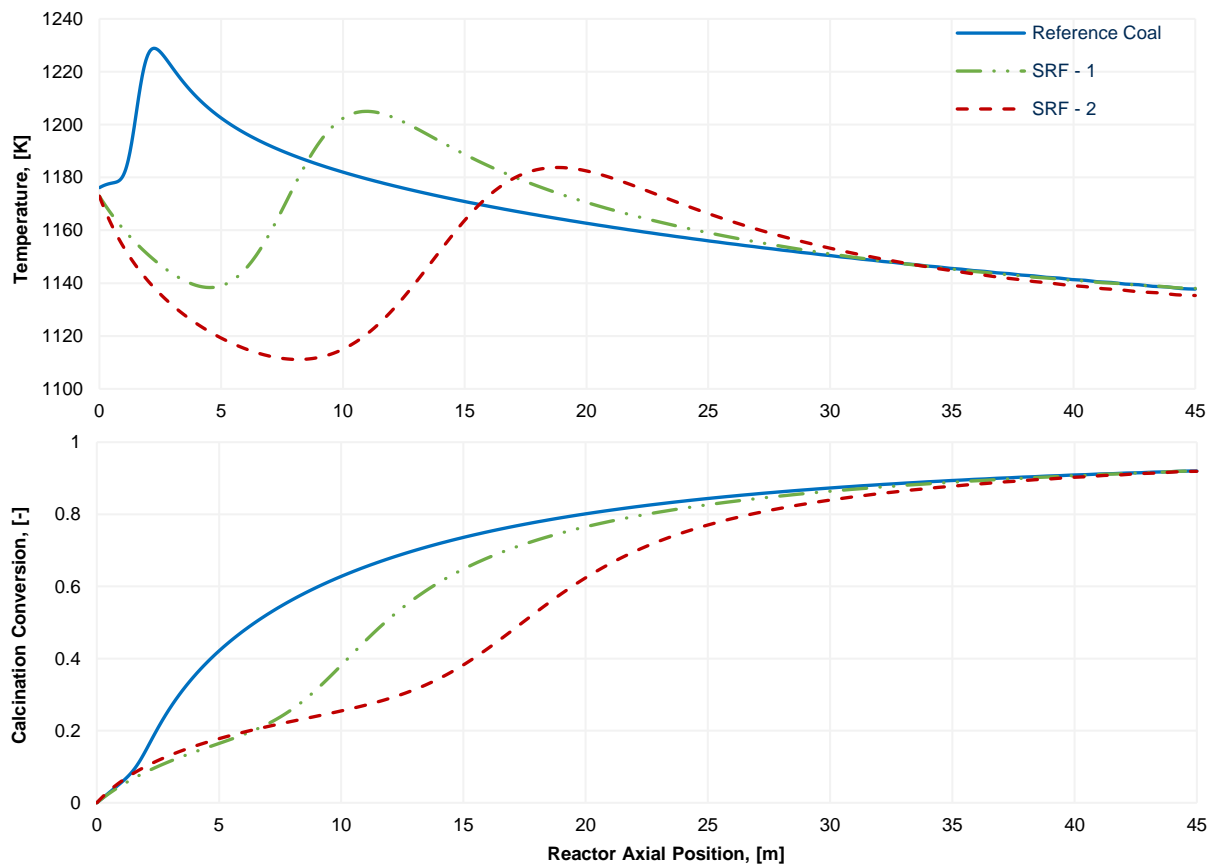
Figure 3: Comparison of temperature and conversion calciner profiles for the reference coal (50μm), SRF-1 (250μm) and SRF-2 (750 μm).

since the length of the calciner is kept constant due to design restrictions.

Table 3 presents the conditions of the flue gas out of the calciner and the preheating tower for the coal and the SRF cases respectively. The concentration of CO_2 in the SRF-case flue gas is lower than the base case, while the oxygen and water concentrations are significantly higher. This is attributed to the very high moisture content of the SRF (7% in comparison with 0.5% for coal) which is transferred to the gas phase and the increased hydrogen to carbon ratio. In addition, the oxygen content of the SRF (33%) is significantly higher in comparison with coal (9%). It is also important to note that the total mass flowrate of flue gas is higher, since more moisture and oxygen are transferred from the solid fuel to the gas phase.

Table 4 summarises and compares the most important KPIs for both the calciner and the kiln systems in terms of specific CO_2 intensity. It is important to note that the fossil-fuel emissions in the calciner for the SRF cases are reduced by 78%. Moreover, it should be borne in mind that even though the substitution rate of coal in the calciner is 100%, there are still some fossil emissions related

to the non-biogenic part of the Solid Recovered Fuel (around 20%). The overall plant's emissions are reduced by 18.5%.

Table 3: Exhaust Gas Conditions for Coal and SRF Cases.

Calciner Exhaust Gas	Coal	SRF
Mass Flowrate (kg/s)	63.3	64.0
Temperature (°C)	865	864
O_2 (v/v wet basis)	2.8	4.4
N_2 (v/v wet basis)	59.2	57.4
CO_2 (v/v wet basis)	33.1	30.6
H_2O (v/v wet basis)	4.9	7.5
Preheating Tower Exhaust Gas	**Coal**	**SRF**
Mass Flowrate (kg/s)	66.2	66.8
Temperature (°C)	315	323
O_2 (v/v wet basis)	3.4	5.0
N_2 (v/v wet basis)	58.9	57.3
CO_2 (v/v wet basis)	31.4	29.0
H_2O (v/v wet basis)	6.2	8.7

Table 4: Important KPIs.

Calciner	Coal	SRF
Process Emissions (kg_{CO2} / $ton_{clinker}$)	510.3	510.3
Fossil-Fuel Emissions (kg_{CO2} / $ton_{clinker}$)	181.3	26.2
Rotary Kiln	**Coal**	**SRF**
Process Emissions (kg_{CO2} / $ton_{clinker}$)	35.0	35.0
Fossil-Fuel Emissions (kg_{CO2} / $ton_{clinker}$)	112.3	112.3
Total Emissions (kg_{CO2} / $ton_{clinker}$)	838.9	683.8

CONCLUSIONS

This study highlights the importance of process modelling and simulation to accurately predict and evaluate the performance of a cement plant burning sustainable biogenic fuels instead of the conventional pulverized coal. Even though the quality (moisture, particle size, heating value) of such fuels is rather poor and the thermal performance of the plant decreases significantly, the overall CO_2 emissions showed a reduction of around 18.5%, just by replacing the fuel in the calciner. Apart from the energy penalty due to the significantly higher moisture content of the SRFs, the implementation of such a technology would also require increased capital investments, since SRF requires higher residence times (equipment) to combust completely. The flue gas out of an SRF-fired calciner has lower CO_2 and higher H_2O and O_2 content, making it more difficult to capture in a post-combustion unit.

ACKNOWLEDGEMENTS

REFERENCES

1. Fennell, P., Driver, J., Bataille, C., & Davis, S. J. (2022). Cement and steel—nine steps to net zero. *Nature*, *603*(7902), 574-577.
2. Bhatty, J. I., Miller, F. M., & Bohan, R. P. (2011). *Innovations in Portland Cement Manufacturing* (2nd ed.). Portland Cement Association. Skokie, Illinois
3. Schneider, M., Hoenig, V., Ruppert, J., & Rickert, J. (2023). The cement plant of tomorrow. *Cement and Concrete Research*, *173*, 107290.
4. Wang, G., Silva, R. B., Azevedo, J. L. T., Martins-Dias, S., & Costa, M. (2014). Evaluation of the combustion behaviour and ash characteristics of biomass waste derived fuels, pine and coal in a drop tube furnace. *Fuel*, *117*, 809-824.
5. Varnier, L., d'Amore, F., Clausen, K., Melitos, G., de Groot, B., & Bezzo, F. (2025). Combined electrification and carbon capture for low-carbon cement: techno-economic assessment of different designs. *Journal of Cleaner Production*, 145029.
6. Mujumdar, K. S., Ganesh, K. V., Kulkarni, S. B., & Ranade, V. V. (2007). Rotary Cement Kiln Simulator (RoCKS): Integrated modeling of pre-heater, calciner, kiln and clinker cooler. *Chemical Engineering Science*, *62*(9), 2590-2607.
7. Gupta, A. V. S. S. K. S., & Nag, P. K. (2000). Prediction of heat transfer coefficient in the cyclone separator of a CFB. *International journal of energy research*, *24*(12), 1065-1079.
8. Mikulčić, H., Von Berg, E., Vujanović, M., Priesching, P., Perković, L., Tatschl, R., & Duić, N. (2012). Numerical modelling of calcination reaction mechanism for cement production. *Chemical engineering science*, *69*(1), 607-615.
9. Iliuta, I., Dam-Johansen, K., & Jensen, L. S. (2002). Mathematical modeling of an in-line low-NOx calciner. *Chemical engineering science*, *57*(5), 805-820.
10. Mikulčić, H., Von Berg, E., Vujanović, M., Wang, X., Tan, H., & Duić, N. (2016). Numerical evaluation of different pulverized coal and solid recovered fuel co-firing modes inside a large-scale cement calciner. *Applied energy*, *184*, 1292-1305.
11. Bisulandu, B. J. R. M., & Huchet, F. (2023). Rotary kiln process: An overview of physical mechanisms, models and applications. *Applied Thermal Engineering*, *221*, 119637.
12. Pieper, C., Liedmann, B., Wirtz, S., Scherer, V., Bodendiek, N., & Schaefer, S. (2020). Interaction of the combustion of refuse derived fuel with the clinker bed in rotary cement kilns: A numerical study. *Fuel*, *266*, 117048.
13. Csernyei, C., & Straatman, A. G. (2016). Numerical modeling of a rotary cement kiln with improvements to shell cooling. *International Journal of Heat and Mass Transfer*, *102*, 610-621.
14. Campanari, S., Cinti, G., Consonni, S., Fleiger, K., Gatti, M., Hoppe, H., Martínez, I., Romano, M., Spinelli, M., & Voldsund, M. (2016). *Design and performance of CEMCAP cement plant without CO_2 capture. CEMCAP Deliverable D4.1.*